Thin Solid Films 595 (2015) 239–243

Contents lists available at ScienceDirect

Thin Solid Films

journal homepage: www.elsevier.com/locate/tsf

Gas-phase reaction kinetics of 1,3-disilacyclobutane in a hot-wire chemical vapor deposition reactor

I. Badran, Y.J. Shi *

Department of Chemistry, University of Calgary, Calgary, Alberta T2N 1N4, Canada

ARTICLE INFO

Article history:
Received 31 January 2015
Received in revised form 30 June 2015
Accepted 30 June 2015
Available online 2 July 2015

Keywords:
1,3-Disilacyclobutane
Reaction kinetics
Hot-wire chemical vapor deposition
Activation energies

ABSTRACT

The reaction kinetics of the decomposition of 1,3-disilacyclobutane (DSCB) was investigated using a hot-wire chemical vapor deposition reactor. The reaction products were monitored using a vacuum ultraviolet laser single-photon ionization source coupled with a time-of-flight mass spectrometer. Steady-state approximation was used to determine the rate constants for three main decomposition pathways of DSCB: the exocyclic H_2 elimination (k_1), the cycloreversion (k_2), and the ring-opening via 1,2-H shift (k_3). Separate k_2 and k_3 were not obtained, but $2k_2 + k_3$ and k_1 were determined. The activation energy (E_a) for the exocyclic H_2 elimination reaction was determined to be 63.5 kJ·mol^{-1}. Compared to the E_a value of 43.6 kJ·mol^{-1} previously obtained under collision-free conditions at much lower pressures, the value from this work is higher. This is attributed to the filament aging caused by the formation of silicon carbide (SiC) and tungsten sub-carbide (W_2C) on the wire surface. The heterogeneous reactions on the metal surface also led to a much faster decay constant, $k_{overall}$, for DSCB than those for each individual decomposition pathway, k_1 and $2k_2 + k_3$.

1. Introduction

Thin films of silicon carbides (SiC) possess superior mechanical and electronic properties that allow them to be used as window layers in solar cells, as well as in many high-power and high-temperature applications. Hot-wire chemical vapor deposition (HWCVD) has emerged as a well-versed technique that can deposit high-quality SiC thin films. 1,3-Disilacyclobutane (DSCB) is considered as a promising single-source precursor for SiC thin film materials using CVD methods [1–3] due to the built-in 1:1 Si:C stoichiometry that matches the one in SiC. Recently, we have investigated the decomposition chemistry of DSCB when it is used as a precursor gas in a HWCVD reactor [4]. It was found that ring stabilization in DSCB as compared to its monosilacyclobutane analogues promoted exocyclic bond cleavages, which mainly led to the formation of a cyclic silylene, i.e., 1,3-disilacyclobut-1-ylidene, and molecular hydrogen (Eq. (1)).

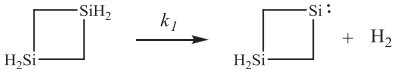

(1)

In addition to the exocyclic H_2 elimination, DSCB was shown to undergo cycloreversion to form two silenes (Eq. (2)), as well as a 1,2-H shift-initiated ring opening to form two pairs of silene and silylene species (Eq. (3)).

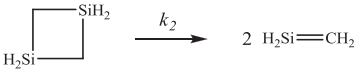

(2)

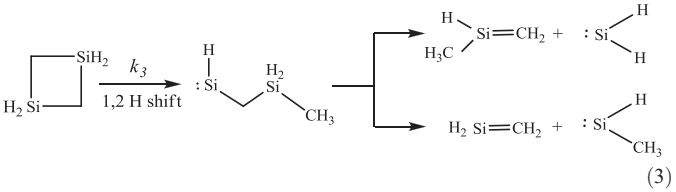

(3)

Our ab initio calculations indicated the dominance of the ring opening of DSCB initiated by 1,2-H shift over the cycloreversion reactions, both kinetically and thermodynamically at 0 and 298 K [5]. We also calculated various H_2 elimination pathways, including both the stepwise and concerted 1,1-, 1,2-, and 1,3-H_2 elimination reactions using the second-order Møller–Plesset (MP2) perturbation theory and the coupled cluster methods with single, double, and perturbative triple excitation (CCSD(T)). At the CCSD(T)/6-311++G(3d,2p) //MP2/6-311++G(d,p) level of theory, the concerted 1,1-H_2 elimination has only slightly higher activation barrier (62.2 kcal·mol^{-1}, i.e., 260 kJ·mol^{-1}) than that of the 1,2-H shift-initiated ring opening reaction (59.9 kcal·mol^{-1}, i.e., 251 kJ·mol^{-1}), therefore the 1,1-H_2 elimination route is kinetically competitive with the ring opening via 1,2-H shift.

* Corresponding author.
E-mail address: shiy@ucalgary.ca (Y.J. Shi).

http://dx.doi.org/10.1016/j.tsf.2015.06.055
0040-6090/

To implement DSCB molecules as precursor gases at the industrial scale for the SiC thin film formation using HWCVD, information is desired on chemical kinetics of the gas-phase reactions responsible for the film deposition. Our previous work on the mechanistic studies [4] and theoretical calculations [5] of the major decomposition pathways has paved the way for us to determine experimentally the rate constants for each pathway, which is the purpose of this work. We have also studied the dependence of rate constants on temperature, from which the activation energies (E_a) for individual decomposition pathway are determined. A comparison of the obtained E_a values in this work with those under the collision-free setup from our previous study [4] helps answer the question whether the reactions in the HWCVD reactor are governed by heterogeneous reactions on the hot-wire surface or the reactions in the gas phase. The outcome of this study will help construct a kinetic model for DSCB when they are used in a HWCVD reactor. This is crucial for their future industrial applications, since both the efficiency and profitability of the process relies heavily on knowledge of the rates of chemical reactions in the gas phase and their dependence on parameters such as concentration and temperature.

2. Experimental details

The experimental setup of the HWCVD reactor and the laser ionization time-of-flight (TOF) mass spectrometer (MS) used in this work has been described elsewhere [6–8]. Briefly, a 10-cm long tungsten filament (D = 0.5 mm, 99.9+%, Aldrich) was placed in a stainless steel HWCVD reactor, connected to a linear TOF mass spectrometer (R. M. Jordan) via a 0.15 mm diameter pinhole. The filament was resistively heated using a DC power supply (Agilent, N5744A) and its surface temperature was measured by a two-color IR pyrometer (Chino Works). The filament temperature was controlled and recorded using LabView®. Gaseous mixtures of DSCB and helium (99.999%, Praxair) were introduced into the reactor using a mass flow controller (MKS, type 1179A). The pressures inside the reactor were monitored by a capacitance manometer (MKS Baratron, type 626A). The chemical species produced from gas-phase reactions in the HWCVD reactor were detected by a nonresonant single-photon ionization (SPI) using 118 nm VUV (10.5 eV) photons in tandem with the TOF mass spectrometer. The VUV laser radiation was generated by frequency tripling the 355 nm UV output of a commercial Nd:YAG laser (Spectra Physics, Lab 170-10) in a gas cell containing 2.80×10^4 Pa (i.e., 210 Torr) of a 10:1 Ar/Xe gas mixture.

DSCB was synthesized by reducing 1,1,3,3-tetrachloro-1,3-disilacyclobutane (TCDSCB) with $LiAlH_4$ (Alfa Aesar, powder, 97%) according to a previously reported method [9]. TCDSCB was prepared by reacting 1,1,3,3-tetraethoxy-1,3-disilacyclobutane (Starfire systems) with acetyl chloride (Sigma-Aldrich, ≥99%) and ferric chloride (Sigma-Aldrich, 97%) following the method proposed by Shen [10]. The structure and purity of DSCB (>98%) were checked by ^{1}H NMR (nuclear magnetic resonance), ^{13}C NMR, gas chromatography–mass spectrometry, and our in-house TOF MS analysis. Diluted gaseous samples of DSCB in helium were prepared by entraining the room-temperature DSCB vapor in helium after degassing its liquid sample through several cycles of 'freeze–pump–thaw'.

A fresh filament was used for each kinetic run at a specified temperature and pressure. The filament was etched using 1.33×10^3 Pa (i.e., 10 Torr) of 10% H_2/He mixture at 2000 °C for 60 min before introducing the sample gas. Filament temperatures in the range of 1000–1300 °C were studied at increments of 50 °C. The total pressure was kept constant at 2.00×10^3 Pa (i.e., 15 Torr). In each kinetic run, a mass spectrum was collected every 1–2 min after the filament was turned on for a period up to 60 min. A calibration curve to relate the peak intensity to its concentration was constructed for each kinetic run by recording the room-temperature mass spectra of 1% DSCB in He in the reactor at each of the pressures of 6.67×10^2 Pa, 1.33×10^3 Pa, 2.00×10^3 Pa, 2.67×10^3 Pa, and 3.33×10^3 Pa. This corresponds to 6.67 Pa, 13.3 Pa, 20.0 Pa, 26.7 Pa, and 33.3 Pa of DSCB when 1% DSCB/He mixture is used. Assuming ideal gas behavior, the concentration of a given species, X, in units of mol·L^{-1} was calculated by the following formula:

$$[X] = \frac{Int(X) \cdot m + n}{RT} \tag{4}$$

where $Int(X)$ is the peak intensity of the species X, m and n are the slope and the intercept of the calibration line, R is the universal gas constant, and T is room temperature. Filament-off mass spectra of the actual reaction samples were recorded to obtain the initial concentration of DSCB. In addition, Eq. (4) was also used to calculate the concentrations of the stable gaseous products formed from the gas-phase reactions. This is reasonable since the ionization cross sections tend to be uniform from molecule to molecule for single-photon ionization using a VUV photon due to its non-resonant nature [11,12].

The rate constants for the main decomposition pathways for DSCB were determined by applying the steady-state approximation (SSA) to the reactive intermediates (e.g., silenes or silylenes) in the reaction mechanism. This allows for the calculation of the rate constant for a given decomposition pathway (e.g., k_1, k_2, and k_3) in terms of the steady-state rates of formation of the stable products [13,14]. For example, consider that a reactant A decomposes into the stable products, B, C, and D, following a multi-step mechanism, the rate constant (k_i) can be given by:

$$k_i = \frac{bR_B^{ss} + cR_C^{ss} + dR_D^{ss}}{a[A]} \tag{5}$$

where R_B^{ss}, R_C^{ss} and R_D^{ss} are the steady-state rates of formation of products B, C and D, respectively, and the coefficients a, b, c and d, are constants derived by applying the SSA to the proposed mechanism. The steady-state rates of formation (R^{ss}) were determined by plotting the concentration in mol·L^{-1} for each of the main stable products as a function of reaction time in seconds. In most of the experiments performed in this work, an initial rise in the concentration of the stable products was observed, followed by a decrease due to the aging of filaments by metal alloy formation. R^{ss} was obtained by linear fitting of the rising part in the plot.

3. Results and discussion

3.1. Determining the gas temperature inside the HWCVD reactor

In order to estimate the activation energies for the major decomposition pathways, the gas temperature inside the HWCVD reactor need to be determined. As proposed by Mankelevich et al. [15], the gas temperature, $T(r)$, as function of the distance (r) away from a hot filament can be modeled by:

$$T(r) = T_{nf}\left[1-\left(T_L/T_{nf}\right)^2 \ln\left(r/R_f\right)/\ln\left(L/R_f\right)\right]^{1/2} \tag{6}$$

where T_{nf} and T_L are the gas temperatures near the filament and at a fixed distance L from the filament, respectively. r is a variable representing the distance from the filament surface, and R_f is the filament radius. Good agreements were shown between the gas-phase temperature calculated using Eq. (6) and those from experimental measurements in HWCVD reactors [16–18]. For T_L and L, it is possible to use the substrate temperature and the filament-substrate gap, respectively [15]. In our reactor, this gap was represented by the distance between the filament and the small pinhole connecting the reactor to the ionization chamber, and it was equal to 5 cm. The temperature of the HWCVD reactor wall was measured in our experiments using a type-K thermocouple. The wall temperature has increased

from ca. 293 to 303 K over the 60-min period when the filament temperature (T_f) was fixed at 1473 K (i.e., 1200 °C). Therefore, T_L was taken to be 298 K. According to previous studies in the literature [16,19,20], the near-filament temperature (T_{nf}) was estimated to be 500 K lower than T_f when $T_f = 2700$ K. In this work, the filament temperatures tested are much lower at 1273–1573 K, therefore T_{nf} was considered to be equal to $T_f - 250$ K. By integrating Eq. (6) over the filament-pinhole distance of 5 *cm*, and averaging the definite integral according to Eq. (7), the average gas temperatures corresponding to each T_f in the range of 1273–1573 K were obtained.

$$\overline{T} = \frac{1}{b-a}\int_a^b T(r)dr \tag{7}$$

where a and b are 0 and 5 cm, respectively. Values of the average gas temperatures corresponding to each T_f are listed in Table 1.

3.2. Rate constant expressions

The kinetics of the decomposition reactions of DSCB were studied based on the reaction mechanism proposed in our previous work on its decomposition chemistry in the HWCVD reactor [4]. The three main decomposition pathways were found to be the formation of 1,3-disilcuclobut-1-ylidene (Eq. (1)), the cycloreversion to form two silenes (Eq. (2)), and the ring-opening via 1,2-H shift (Eq. (3)). Under the operating DSCB pressures of 16.0–64.0 Pa in the reactor, four major stable products of 1-methyl-1,3-disilacyclobutane (102 amu), 1-silyl-1,3-disilacyclobutane (118 amu), 1-methylsilyl-1,3-disilacyclobutane (132 amu), and 1,1′-bis(1,3-disilacyclobutane) (174 amu) were detected. Among them, only the peak intensities of m/z 102 and 174 are sufficiently strong to obtain reliable steady-state rates of formation for the two products. The formation of the product of 1,1′-bis(1,3-disilacyclobutane) (174 amu) involves the insertion of 1,3-disilcuclobut-1-ylidene into the Si–H bond in DSCB (Eq. (8)), whereas 1-methyl-1,3-disilacyclobutane (102 amu) originates from the cycloaddition reaction of silene and methylsilene (Eq. (9)) [4].

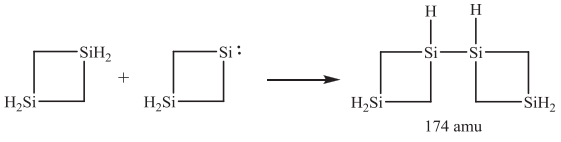

(8)

Table 1
Average gas temperatures (T_{gas}) in the HWCVD reactor for different filament temperatures (T_f) and the rate constants for the decomposition reactions of DSCB at a reactor pressure of 2.00×10^3 Pa and various T_f's.

T_f (K)	T_{gas} (K)	$k_1 \times 10^5$ (s^{-1})	$(2k_2 + k_3) \times 10^5$ (s^{-1})	$k_{overall} \times 10^5$ (s^{-1})
1273	584	0.473	1.01	151
1323	605	1.21	–[a]	320
1373	625	2.57	0.667	317
1423	646	–[a]	–[a]	701
1473	669	2.63	2.28	399
1523	687	–[a]	1.89	977
1573	708	6.55	1.01	844

[a] Some values of k_1 and $2k_2 + k_3$ were not reported due to the inability to obtain R^{ss}_{174} and R^{ss}_{102}.

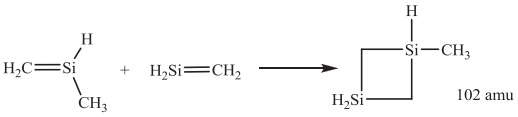

(9)

Applying the steady-state approximation to the intermediates involved in the proposed mechanism (including Eqs. 1–3, 8, and 9), the rate constants k_1 (H_2 elimination), k_2 (cycloreversion), and k_3 (ring opening via 1,2-H shift) can be expressed by the following three equations.

$$k_1 = \frac{R^{ss}_{174}}{[DSCB]} \tag{10}$$

$$k_2 = \frac{R^{ss}_{102} - 2\Phi R^{ss}_{102}}{2(1-\Phi)\,[DSCB]} \tag{11}$$

$$k_3 = \frac{R^{ss}_{102}}{(1-\Phi)\,[DSCB]} \tag{12}$$

where R^{ss}_{102} and R^{ss}_{174} represent the steady-state rate of formation of the stable products with a mass of 102 amu and 174 amu, respectively, [DSCB] is the concentration of DSCB, and Φ is the branching ratio to produce $H_2Si = CH_2$ in reaction (3). Separate expressions for k_2 and k_3 could not be derived since the branching ratio, Φ, is not known.

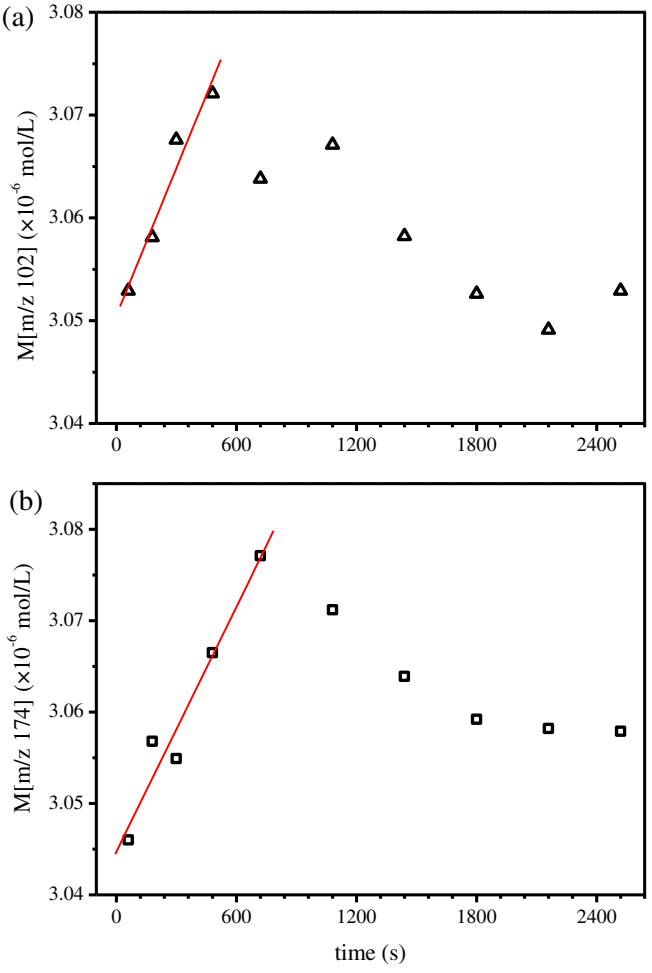

Fig. 1. Plots of the concentration vs. time to determine the rates of formation of the stable products at (a) *m/z* 102, and (b) *m/z* 174 from 2.00×10^3 Pa of 1% DSCB in He in the HWCVD reactor at a W filament temperature of 1273 K.

However, from Eqs. (11) and (12), an expression for $2k_2 + k_3$ can be obtained in terms of R^{ss}_{102} and [DSCB].

$$2k_2 + k_3 = \frac{2R^{ss}_{102}}{[DSCB]} \quad (13)$$

Fig. 1 shows the typical plots of product concentration vs. reaction time for obtaining the rates of formation for the two products at $T_f =$ 1273 K. From the obtained values of R^{ss}_{102} and R^{ss}_{174}, the rate constants of k_1 and $2k_2 + k_3$ can be determined.

3.3. The temperature dependence of the rate constants of DSCB decomposition reactions

The effect of temperature on the kinetics of the DSCB decomposition reactions was studied in the filament temperature range of 1273–1573 K, which corresponds to a gas temperature ranging from 584 to 708 K. The experiments were performed at a fixed total pressure of 2.00×10^3 Pa for the 1% DSCB/He mixture in the reactor. DSCB kinetics was dramatically fast at T_f greater than 1573 K due to the dominance of the DSCB-filament surface reactions, therefore, T_f's beyond 1573 K were not explored. The values of rate constants k_1 and $2k_2 + k_3$ for the three main decomposition pathways of DSCB, represented in Eqs. (1) to (3) and determined from the steady-state rates of formation for the stable products as explained in the previous section, are listed in Table 1. In the experiments performed using 1% DSCB/He samples in the reactor at constant T_f's, the DSCB peak intensity showed a fast decay, which obeyed first-order kinetics. Fig. 2 shows a typical plot of the natural logarithm of the DSCB peak intensity, I(m/z 88). The values of overall first-order decay constant ($k_{overall}$) at different temperatures are also tabulated in Table 1.

The rate constant of H_2 elimination reaction from DSCB, k_1, showed an Arrhenius behavior within the temperature range 1273–1573 K at a reactor pressure of 2.00×10^3 Pa (Fig. 3). The activation energy, E_a, for the H_2 elimination was determined to be 63.5 kJ·mol^{-1}. In our previous work on studying the decomposition mechanism of DSCB on the hot W filament [4], we were able to determine the E_a value for the formation of molecular hydrogen on a W wire to be 43.6 kJ·mol^{-1}. This value was obtained under the collision-free conditions, where the reactions in the gas phase were not possible to occur. The dissociation of DSCB on the hot W surfaces follows a dissociative adsorption mechanism where the rate-determining step (RDS) is the initial Si–H bond rupture on the surface [7,21]. Due to the much higher pressures, the reactions in the HWCVD setup, that were studied in this work, are more complex involving both the heterogeneous reactions on the metal surfaces and the reactions in the gas phase. Fig. 4 shows a comparison between the activation energy obtained in this study and those obtained in the collision-free experiments [4], in pyrolysis [22], and in theoretical calculations [5]. The E_a value for the 1,1-H_2 elimination obtained from this kinetic study at 63.5 kJ·mol^{-1} in the reactor setup is higher than 43.6 kJ·mol^{-1} determined from the collision-free setup. Two reasons could contribute to this difference: 1) there is a contribution from the concerted molecular elimination of H_2 in the gas phase, which requires higher activation energy; 2) the structure of W filament is changed after exposure to DSCB, leading to an increase in the activation energy. The activation enthalpy for the concerted 1,1-H_2 elimination from DSCB in the gas-phase was calculated to be 62.2 kcal·mol^{-1} (i.e., 260 kJ·mol^{-1}) [5], which is not consistent with the determined value of 63.5 kJ·mol^{-1}. Therefore, the contribution from the gas-phase molecular elimination of H_2 can be discounted. From our examination on the structures of W filaments after being exposed to DSCB source gases, we found that crystalline SiC and tungsten sub-carbide (W_2C) were formed on the W wire surface in the filament temperature range studied in this work. This provides strong support that the structural change in W filament, or filament

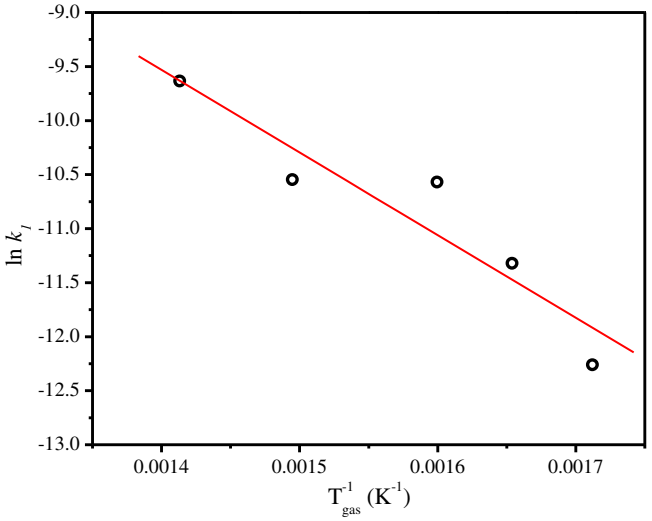

Fig. 3. Arrhenius plot for the exocyclic H_2 elimination reaction for 1% DSCB at a reactor pressure of 2.00×10^3 Pa.

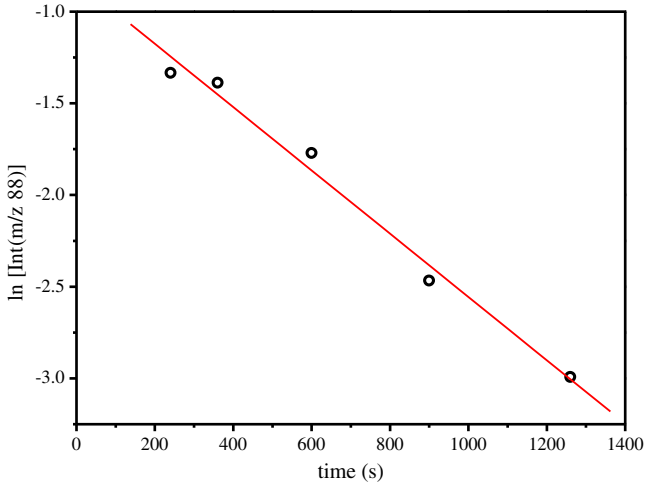

Fig. 2. The 1st order decay of DSCB peak intensity at a W filament temperature of 1273 K.

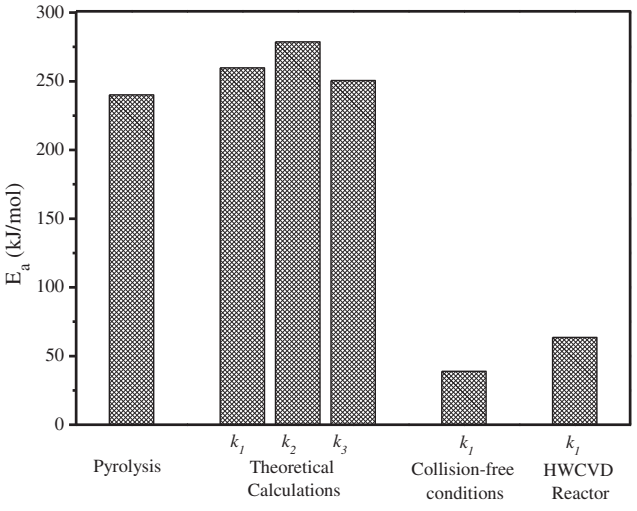

Fig. 4. Comparison of the activation energies of DSCB decomposition reactions determined from experiments (a) using a HWCVD reactor (this work), (b) under collision-free conditions (Ref. [4]), (c) pyrolysis (Ref. [20]), and (d) from theoretical calculations (Ref. [5]).

aging, causes an increase in the activation energy for the H_2 elimination reaction in the reactor setup as compared to the value determined from the low-temperature collision-free conditions. This agrees with a previous study that also showed an increase in the activation energy for the production of SiH_3 radicals from SiH_4 decomposition on W wires due to the formation of W_5Si_3 on the metal wires after exposure to SiH_4 [23]. Although the E_a value for the H_2 elimination reaction is higher in the reactor setup, it is still much lower than the theoretical value (260 kJ·mol^{-1}). This suggests that the SiC or W_2C still catalyzes the H_2 elimination, although they are not as good a catalyst as the W metal itself.

As shown in Table 1, the rate constant for the overall decay of DSCB, $k_{overall}$, is much higher than those of the individual decomposition pathways, k_1 and $2k_2 + k_3$. This is mainly due to reactions of DSCB and its decomposition products with the W filament to form metal carbide and silicon carbide on the wire surface, as discussed above. Auner et al. studied the pyrolysis of DSCB in a low-pressure flow system in the temperatures ranging from 516 to 573 °C [22]. It was found that the primary reaction in the pyrolysis was the ring opening initiated by 1,2-H shift (Eq. (3)) to form silylene and silene species. In the presence of H_2, monomethylsilane and dimethylsilane were formed as the major products detected. The E_a for the overall decomposition of DSCB by the pyrolysis was determined to be 230 kJ·mol^{-1}, also shown in Fig. 4. This E_a value is close to the calculated one at 59.9 kcal·mol^{-1} (i.e., 251 kJ·mol^{-1}) using ab initio methods for the ring opening reaction [5]. This is in agreement with the claim that the main decomposition route in pyrolysis is the 1,2-H shift-initiated ring-opening reaction. Unfortunately, from the determined $2k_2 + k_3$, the E_a value for route 3 (ring opening) cannot be obtained, making it impossible to compare with the pyrolysis value.

4. Conclusions

The reaction kinetics of DSCB was studied under practical HWCVD pressures and temperatures in a reactor setup. The steady-state approximation (SSA) method was employed to deduce the rate constants for the main decomposition pathways for DSCB in terms of the rates of formation for the stable products. From this, the rate constant for the DSCB decomposition to form H_2, k_1, was determined. The rate constants for the other two decomposition channels, cycloreversion (k_2) and 1,2-H shift-initiated ring opening reaction (k_3), were determined in the form of $2k_2 + k_3$. In addition, the first-order decay constants for DSCB, $k_{overall}$, were obtained. The temperature dependence of these rate constants was investigated in the T_f range of 1273–1573 K. The activation energies for the H_2 elimination reaction for DSCB was determined to be 63.5 kJ·mol^{-1} in the reactor setup where the total pressure is maintained at 2.00×10^3 Pa. This E_a value is much higher than the one obtained previously at 43.6 kJ·mol^{-1} under collision-free conditions at much lower pressures, and this is due to the filament aging caused by the formation of SiC and W_2C on the wire surface. The heterogeneous reactions on the metal surface also led to a much faster decay constant for DSCB than those for each individual decomposition pathway, k_1 and $2k_2 + k_3$. The importance of this kinetic study is two-fold. On one hand, it shapes a methodology to study the kinetics of the complex reactions involved in the HWCVD reactor. Using this method, it was possible to determine the rate constants for the decomposition reactions in the reactor setup and their corresponding E_a values. On the other hand, the data provided in this work can contribute to the construction of a kinetic model for using DSCB as a source gas in an industrial HWCVD reactor.

Acknowledgments

The financial support from the Natural Sciences and Engineering Council of Canada (NSERC) via the Discovery Grant, the Canadian Foundation for Innovation (CFI) via the New Opportunities Fund, and the University of Calgary for this work is gratefully acknowledged.

References

[1] D.J. Larkin, L.V. Interrante, Chemical vapor deposition of silicon carbide from 1,3-disilacyclobutane, Chem. Mater. 4 (1992) 22–24.
[2] A.K. Chaddha, J.D. Parsons, J. Wu, H.S. Chen, D.A. Roberts, H. Hockenhull, Chemical vapor deposition of silicon carbide thin films on titanium carbide using 1,3 disilacyclobutane, Appl. Phys. Lett. 62 (1993) 3097–3098.
[3] Z. Bastl, H. Bürger, R. Fajgar, D. Pokorná, J. Pola, M. Senzlober, J. Šubrt, M. Urbanová, Si/C phases from the IR laser-induced decomposition of silacyclobutane and 1,3-disilacyclobutane, Appl. Organomet. Chem. 10 (1992) 83–99.
[4] I. Badran, Y.J. Shi, Promotion of exocyclic bond cleavages in the decomposition of 1,3-disilacyclobutane in the presence of a metal filament, J. Phys. Chem. A 119 (2015) 590–600.
[5] I. Badran, A. Rauk, Y.J. Shi, Theoretical study on the ring-opening of 1,3-disilacyclobutane and H_2 elimination, J. Phys. Chem. A 116 (2012) 11806–11816.
[6] I. Badran, T.D. Forster, R. Roesler, Y.J. Shi, Competition of silene/silylene chemistry with free radical chain reactions using 1-methylsilacyclobutane in the hot-wire chemical vapor deposition process, J. Phys. Chem. A 116 (2012) 10054–10062.
[7] Y.J. Shi, Acc. Chem. Res. 48 (2015) 163–173.
[8] Y.J. Shi, X.M. Li, R. Toukabri, L. Tong, Effect of Si–H bond on the gas-phase chemistry of trimethylsilane in the hot wire chemical vapor deposition process, J. Phys. Chem. A 115 (2011) 10290–10298.
[9] R.M. Irwin, J.M. Cooke, J. Laane, Ring conformation and barrier to inversion of 1,3-disilacyclobutane from low-frequency vibrational spectra, J. Am. Chem. Soc. 99 (1977) 3273–3278.
[10] Q.H. Shen, L.V. Interrante, Structural characterization of poly(silylenemethylene), Macromolecules 29 (1996) 5788–5796.
[11] U. Schühle, J.B. Pallix, C.H. Becker, Sensitive mass spectrometry of molecular adsorbates by stimulated desorption and single-photon ionization, J. Am. Chem. Soc. 110 (1988) 2323–2324.
[12] Y.J. Shi, X.K. Hu, D.M. Mao, S.S. Dimov, R.H. Lipson, Analysis of xanthate derivatives by vacuum ultraviolet laser time-of-flight mass spectrometry, Anal. Chem. 70 (1998) 4534–4539.
[13] S.H. Mousavipour, P.D. Pacey, Initiation and abstraction reactions in the pyrolysis of acetone, J. Phys. Chem. 100 (1996) 3573–3579.
[14] S.H. Mousavipour, V. Saheb, S. Ramezani, Kinetics and mechanism of pyrolysis of methyltrichlorosilane, J. Phys. Chem. A 108 (2004) 1946–1952.
[15] Y.A. Mankelevich, A.T. Rakhimov, N.V. Suetin, Two-dimensional simulation of a hot-filament chemical vapor deposition reactor, Diam. Relat. Mater. 5 (1996) 888–894.
[16] L. Schafer, C.P. Klages, U. Meier, K. Kohsehoinghaus, Atomic-hydrogen concentration profiles at filaments used for chemical vapor deposition of diamond, Appl. Phys. Lett. 58 (1991) 571–573.
[17] K.H. Chen, M.C. Chuang, C.M. Penney, W.F. Banholzer, Temperature and concentration distribution of H_2 and H-atoms in hot filament chemical vapor deposition of diamond, J. Appl. Phys. 71 (1992) 1485–1493.
[18] S.A. Redman, C. Chung, K.N. Rosser, M.N.R. Ashfold, Resonance enhanced multiphoton ionisation probing of H atoms in a hot filament chemical vapour deposition reactor, Phys. Chem. Chem. Phys. 1 (1999) 1415–1424.
[19] J.A. Smith, E. Cameron, M.N.R. Ashfold, Y.A. Mankelevich, N.V. Suetin, On the mechanism of CH_3 radical formation in hot filament activated CH_4/H_2 and C_2H_2/H_2 gas mixtures, Diam. Relat. Mater. 10 (2001) 358–363.
[20] Y.A. Mankelevich, N.V. Suetin, J.A. Smith, M.N.R. Ashfold, Investigations of the gas phase chemistry in a hot filament CVD reactor operating with $CH_4/N_2/H_2$ and $CH_4/NH_3/H_2$ gas mixtures, Diam. Relat. Mater. 11 (2002) 567–572.
[21] R. Toukabri, N. Alkadhi, Y.J. Shi, Formation of methyl radicals from decomposition of methyl-substituted silanes over tungsten and tantalum filament surfaces, J. Phys. Chem. A 117 (2013) 7697–7704.
[22] N. Auner, I.M.T. Davidson, S. Ijadimaghsoodi, F.T. Lawrence, Kinetics and mechanism of pyrolysis of 1,3-disilacyclobutane, 1,3-dimethyl-1,3-disilacyclobutane, and 1,1,3,3-tetramethyl-1,3-disilacyclobutane in the gas phase, Organometallics 5 (1986) 431–435.
[23] J.K. Holt, M. Swiatek, D.G. Goodwin, H.A. Atwater, The aging of tungsten filaments and its effect on wire surface kinetics in hot-wire chemical vapor deposition, J. Appl. Phys. 92 (2002) 4803–4808.